Time Dependent Response to Cooling in a Beta-Plane Basin

by

Joseph Pedlosky*

Department of Physical Oceanography

Woods Hole Oceanographic Institution

Woods Hole, MA 02543

January 3, 2006

*e-mail: jpedlosky@whoi.edu

Abstract

The time dependent response of an ocean basin to the imposition of cooling (or heating) is examined in the context of a quasi-geostrophic, two-layer model on the beta plane. The focus is on the structure and magnitude of the vertical motion and its response to both a switch –on forcing and a periodic forcing.

The model employed is a time dependent version of an earlier model used to discuss the intensification of sinking in the region of the western boundary current. The height of the interface of the two-layer model serves as an analogue of temperature and the vertical velocity at the interface consists of a cross-isopycnal velocity modeled in terms of a relaxation to a prescribed interface height, an adiabatic representation of eddy thickness fluxes parameterized as lateral diffusion of thickness, and the local vertical motion of the interface itself.

The presence of time dependence adds additional dynamical features to the problem, in particular the emergence of low frequency, weakly damped Rossby basin modes. If the buoyancy forcing is zonally uniform the basin responds to a switch on of the forcing by coming into steady state equilibrium after the passage of a single Rossby baroclinic Rossby wave. If the forcing is non uniform in the zonal direction a sequence of Rossby basin modes is excited and their decay is required before the basin achieves a steady state.

For reasonable parameter values the boundary layers in which both the horizontal and vertical circulations are closed are quasi –steady and respond to the instantaneous state of the interior. As in the steady problem the flow is sensitive to small non quasi-geostrophic mass fluxes across the perimeter of the basin. These fluxes generally excite basin modes as well.

The basin modes will also be weakly excited if the beta plane approximation is relaxed.

The response to periodic forcing is also examined and the sensitivity of the response to the structure of the forcing is similar to the switch –on problem.

1. Introduction

In a recent paper (Pedlosky and Spall, 2005, hereafter PS) the buoyancy driven circulation in a beta-plane ocean was examined in the context of a simple quasi-geostrophic two-layer model. The central result of that study was the demonstration of the western intensification of the sinking produced by basin-wide cooling and the concentration of the sinking in very narrow boundary layer regions. In such narrow zones, strongly affected by frictional dissipation, the vorticity produced by the planetary vortex stretching consequent to the strong vertical motion can be dissipated by interaction with the lateral boundary. Of particular interest was the balance of the vertical transport in the interior with the western boundary current that closes the horizontal circulation leaving the net sinking along each latitude circle to occur in an extremely narrow sub-layer on the western boundary. That study and the one reported here are motivated by the important role of buoyancy driven circulations in the high latitude polar oceans, marginal seas and their connection to the thermohaline circulation.

Given the balance of the vertical transports between the interior and boundary layer regions in the steady model, it is natural to inquire about the nature of the balances in situations in which the circulation has not achieved a steady state. In particular, what is the connection between the interior vertical mass flux and that of the boundary regions when the flow responds to changes in the buoyancy forcing, either an abrupt change or a periodic alteration of the forcing? In particular, the role of low frequency, slightly damped baroclinic Rossby basin modes are essential ingredients in the response. These modes and their role in the low frequency dynamics of oceanic basin circulations have

been discussed by several authors, e.g., LaCasce (2000), Cessi and Primeau (2001), LaCasce and Pedlosky (2002), and of especial interest for the present study, Cessi and Louazel, (2001). The more general problem of the time dependent response to buoyancy forcing has been considered in a numerical study by Lucas et. al. (2005).

To examine this question the simple two-layer model of PS is used. The vertical velocity at the interface is modeled as due to a contribution from several distinct mechanisms. First, there is a cross-isopycnal flux across the interface parameterized in terms of the deviation of the interface from a specified, spatially varying height field that represents the external buoyancy forcing. In addition, a lateral diffusion of thickness is explicitly included to parameterize, in the fashion of Gent and McWilliams (1990), the effect of adiabatic eddy fluxes of thickness by the unresolved eddy field in the interior of the basin and as a model of sub mesoscale horizontal mixing in narrow boundary layers. For the time dependent development, the vertical motion of the interface also contributes to the vertical velocity.

In section 2 the quasi-geostrophic model is described and the time dependent problem for the interior is formulated for the switch-on case. Section 3 describes the interior solution and, in particular, the question of whether Rossby basin modes are excited. It is demonstrated that the external buoyancy forcing must contain a zonal variation to excite the modes and in the present study we examine the effect of concentrating the forcing in the eastern part of the basin. This has important implications for the time required to achieve a steady state. The important role of flow across the basin boundary in exciting the Rossby modes is also discussed. Section 4 discusses the boundary layers required to close the circulation and it is shown that the balances in the

boundary layers are quasi-steady; i.e. that time can be treated as a parameter as the boundary layers respond to the instantaneous state of the interior. Section 5 discusses the response of the basin to periodic forcing and the role of resonance in determining the magnitude of the response. Section 6 summarizes the results of the paper and emphasizes the long adjustment times implied by the dynamics, the non-local relation of the vertical motion and the forcing and, again, the narrow regions containing the strongest vertical velocities.

2. The model

The model used in this study is a two – layer, beta-plane, quasi-geostrophic system shown in Figure 1. The motion is purely baroclinic, driven by only a buoyancy forcing and the fluid consists of two layers of slightly different densities separated by an interface whose departure from the horizontal is η(x,y,t) where x and y are coordinates to the east and north respectively and t is time. The dynamics is assumed to be linear. The rest thicknesses of each layer, H_1 and H_2 are equal (H) . The *nondimensional* equations of motion are:

$$b\varepsilon^2 u_t - fv = \eta_x + b\delta_m{}^3\nabla^2 u$$

$$b\varepsilon^2 v_t + fu = \eta_y + b\delta_m{}^3\nabla^2 v \qquad (2.1.a, b, c)$$

$$u_x + v_y = 2w_i$$

Subscripts *t, x, y* denote differentiation with respect to those variables. The motion is purely baroclinic and the velocities appearing in (2.1 a, b, c) are the difference of the velocities between the two layers, i.e. $\vec{u} = \vec{u}_1 - \vec{u}_2$ (this accounts for the factor of 2 in

(2.1.c) The motion is purely baroclinic and the velocities appearing in (2.1 a, b, c) are the difference of the velocities between the two layers, i.e. $\vec{u} = \vec{u}_1 - \vec{u}_2$. The horizontal, baroclinic velocities in the x, and y directions *(u,v)* are scaled with *U (*which will be related to the amplitude of the buoyancy forcing). The horizontal space variables are scaled with *L* which is characteristic of the basin's zonal extent. Time is scaled with the characteristic period of a long Rossby wave whose zonal wavelength is *L* and this scale is $T = L / \beta L_d^{\,2}$ where L_d is the deformation radius, $(g'H)^{1/2} / f_o$ where *g'* is the reduced gravity and f_o is the characteristic value of the Coriolis parameter on the beta plane. The parameters appearing in (1.2 a, b, c) are,

$$b = \frac{\beta L}{f_o}, \qquad \varepsilon = \frac{L_d}{L}, \quad \delta_m = \left(\frac{A}{\beta}\right)^{1/3} / L \tag{2.2 a, b, c}$$

Both ε and δ_m, the non dimensional Munk boundary layer scale, (*A* is the turbulent coefficient of horizontal momentum mixing) are very small parameters. The beta plane parameter *b* is also assumed small although larger than the other two. The Coriolis parameter in (2.1 a, b) is $f = (1 + by)$. The scaling for the interface height η is

$$\eta_{\text{dimensional}} = \frac{f_o UL}{g'} \eta \tag{2.3}$$

The vertical velocity at the interface, w_i, is scaled with *UH/L* . The key feature of the model is the parameterization of this velocity in terms of the interface deviation η. We represent w_i as,

$$w_i = b\left[\eta_t + \frac{\eta - \theta}{\delta_T} - \delta_K \nabla^2 \eta\right] \qquad (2.4)$$

The first term in (2.4) represents the vertical velocity due to the motion of the interface. The second term is a representation of the cross isopycnal velocity due to vertical mixing and is proportional to the difference between the interface height and a specified field $\theta(x,y,t)$ that is the external forcing. Its scaling relation to its dimensional counterpart is the same as the interface height, i.e. as in (2.3) and so that serves to set the scale of the velocity in terms of the amplitude of the buoyancy forcing. This is taken as a crude representation of a vertical mixing process that tends to restore the interface, or temperature, to an equilibrium, θ, determined by atmospheric forcing, The parameter δ_T is the distance, scaled with L, that a baroclinic Rossby wave travels during the decay time γ associated with the vertical mixing, i.e.

$$\delta_T = \frac{\beta L_d^{\,2}}{\gamma L} \qquad (2.5)$$

The final term in (2.4) is the lateral diffusion of layer thickness by unresolved eddy processes with a characteristic diffusion coefficient κ, defining the nondimensional scale,

$$\delta_K = \frac{\kappa}{\beta L_d^{\,2} L} \qquad (2.6)$$

The boundary conditions that are applied to this system are no-slip conditions on the tangential velocity at the basin boundary, thermally insulating conditions there as well, (i.e. that $\hat{n}\bullet\nabla\eta = 0$ on the boundary whose outward normal is $\hat{n}$) and a small O(b) baroclinic outflow (or inflow) is allowed whose total, integrated around the basin's

perimeter, is $\Delta V(t) = b\,\delta V(t)$. The net inflow for the order one (in the parameter b) horizontal flow must be zero since this for this flow the pressure acts as a streamfunction and so the net integrated inflow around the perimeter of the flow vanishes. The first contribution to the *net* inflow must be therefore, an $O(b)$ smaller. Or equivalently, a net inflow drives an order b^{-1} horizontally non divergent flow as a geostrophic response. Since the problem considered here is linear only the relative order of the two orders of flow are important. It is the physical constraint of rotation that makes the horizontal circulation non divergent at lowest order and hence so sensitive to the $O(b)$ net inflow.

In non dimensional units the zonal extent of the rectangular basin is $(0, x_e)$ and its latitudinal extent is $(0, L_y)$. This integral constraint, when combined with (2.1c) and (2.4) yields,

$$\int_0^{L_y} dy \int_0^{x_e} 2w_t dx = \oint_C \vec{u}\bullet\hat{n}dl = b\delta V$$

$$= b(\int_0^{L_y} dy \int_0^{x_e} dx(\eta_t + \frac{[\eta-\theta]}{\delta_T}) + \delta_K \oint_C \hat{n}\bullet\nabla\eta dl) \qquad (2.7)$$

$$= b(\int_0^{L_y} dy \int_0^{x_e} dx(\eta_t + \frac{[\eta-\theta]}{\delta_T})$$

or,

$$dV(t) = \int_0^{L_y}\int_0^{x_e} dxdy\left[\eta_t + \frac{\eta-\theta}{\delta_T}\right] \qquad (2.8)$$

3. The interior response to a buoyancy switch-on.

For small values of $(\varepsilon, \delta_m, \delta_K)$, the interior equations, outside all boundary layers are:

$$-fv = \eta_x$$

$$fu = \eta_y \qquad \text{(3.1.a ,b, c)}$$

$$u_x + v_y = 2w_i$$

while the vertical velocity at the interface is approximated simply as,

$$w_i = b\left[\eta_t + \frac{\eta - \theta}{\delta_T}\right] \qquad \text{(3.1.d)}$$

Eliminating the gradients of the interface height in (3.1.a, b) leads to the planetary vorticity equation ,

$$2fw_i = -bv = b\eta_x / f \qquad \text{(3.2)}$$

so that the interior is in Sverdrup balance, and using this in (3.1.d) leads to the governing equation for η in the interior of the basin, viz.,

$$\frac{1}{f^2}\eta_x - 2\eta_t - 2\eta/\delta_T = -2\theta/\delta_T \qquad \text{(3.3)}$$

The beta plane parameter *b* is small so *f* in (3.3) can be replaced by unity. The buoyancy forcing θ is taken to be a linear function of latitude, increasing northward and so representing a cooling which increases with latitude. The buoyancy forcing is also taken as an exponentially decreasing function of position from the eastern boundary. We will see that the precise variation of θ is less important than the fact that it varies in x and it

seems more realistic to imagine that it varies than that it is absolutely independent of x. Concentration of the forcing near the eastern boundary also allows a clearer picture of the processes required to excite motion in the western boundary layer.

Thus (3.3) becomes,

$$\eta_x - 2\eta_t - 2\eta/\delta_T = -2\theta_o(y)e^{-\mu(x_e-x)}/\delta_T,$$
$$\theta_o(y) = \theta_{oo}(y-y_o)/L_y \qquad \text{(3.4 a,b)}$$

The hyperbolic, first order, equation (3.4.a) must satisfy the following boundary conditions. First, on the *eastern* boundary of the basin where transport boundary layers are not possible the interior solution must have zero zonal velocity or, equivalently, constant η,

$$\eta = N_e(t) \qquad \text{on } x=x_e \qquad (3.5)$$

where N_e is the unknown interface height on the eastern boundary. It is independent of y but is an unknown function of time.

At the same time, the integral condition (2.8) must be satisfied by the interior solution since the correction to the interface deviations in the boundary layers are no larger than in the interior but they occupy an asymptotically small portion of the basin and so contribute terms of, at most, order δ_m and δ_K and so are negligible. Although the solution of (3.4) can be carried out using the method of characteristics the application of (2.8) is more directly carried out if the problem is solved using a Laplace transform.

If we denote the Laplace transform of any variable by a caret symbol, the Laplace transform of η satisfies,

$$\hat{\eta}_x - 2\hat{\eta}(s+\delta_T^{-1}) = \frac{-2\theta_o(y)}{s\delta_T} e^{-\mu X} \tag{3.6}$$

where s is the Laplace transform variable and $X=(x_e-x)$. The solution of (3.6) satisfying (3.5) is,

$$\hat{\eta}(x,y,s) = \frac{\theta_o}{\delta_T s(s-\mu/2+1/\delta_T)}\left[e^{-\mu X} - e^{-2(s+1/\delta_T)X}\right] + \hat{N}_e(s)e^{-2(s+1/\delta_T)X} \tag{3.7}$$

The Laplace transform of the interface height on the eastern boundary is obtained from (2.8). A simple calculation yields,

$$\tilde{N}_e = \frac{\langle\theta_o\rangle / L_y}{\delta_T s\left(s-\mu/2+1/\delta_T\right)} \frac{\left[e^{-\mu x_e} - e^{-2(s+1/\delta_T)x_e}\right]}{\left[1-e^{-2(s+1/\delta_T)x_e}\right]} + \frac{\delta\tilde{V}(s)/L_y}{\left[1-e^{-2(s+1/\delta_T)x_e}\right]} \tag{3.8}$$

where the bracket $\langle\ \rangle$ denotes an integration in y over the interval (0, L_y). Note that if μ is zero the two brackets in the first term on the right hand side of (3.8) cancel. With the interface height on the eastern boundary determined, the interior solution is known. Of course, we use the Laplace transform inversion to obtain the solution in physical space and time. First note that from (3.2) the vertical velocity in the interior is obtained by taking the x derivative of the interface height. That result of that calculation is given in Appendix A.

The inversion of the Laplace transform is easily accomplished. The inversion integral runs parallel to the imaginary *s* axis shifted to the right of any singularity in the transformed variables so that *s* has a positive real part. From (3.7) and (3.8) we note that there is a simple pole at *s* =0 (corresponding to the eventually steady solution) and a pole at $s = \mu / 2 - 1/\delta_T$ which corresponds to a decay of a Rossby wave at a rate $1/\delta_T$ while the part proportional to μ describes the westward advancing shape formed by the forcing. The most interesting aspect of the inversion calculation is the presence of the term $1 - e^{-2(s+1/\delta_T)x_e}$ in the denominator of (3.8) in both the term involving the y average of the buoyancy forcing and the cross-perimeter net flow. There are several ways to treat this factor but the most physically revealing is to note that on the inversion contour with a positive real part to *s* the exponential term is less than one so that the factor can be developed into a convergent Taylor series, i.e.

$$\frac{1}{1 - e^{-2(s+1/\delta_T)x_e}} = \sum_{n=0} e^{-2n(s+1/\delta_T)x_e} \tag{3.9}$$

When combined with a factor like e^{st} in the Laplace inversion integral, this yields a series of Heavyside functions each representing a nondispersive baroclinic Rossby wave traveling across the basin westward from the eastern boundary initiated at the time $t_n = 2nx_e$. The total solution for the interface height in the interior is then,

$$\eta = \frac{\theta_o(y)}{\left(1-\frac{\mu\delta_T}{2}\right)}\left[\left\{e^{-\mu X} - e^{-t/\delta_T}e^{-\mu(X-t/2)}\right\} - \left\{e^{-2X/\delta_T} - e^{-t/\delta_T}e^{-\mu(X-t/2)}\right\}H(t-2X)\right]$$

$$+\frac{\langle\theta_o\rangle / L_y}{\left(1-\frac{\mu\delta_T}{2}\right)}e^{-\mu x_e}\left\{e^{-2X/\delta_T} - e^{-t/\delta_T}e^{-\mu(X-t/2)}\right\}H(t-2X) \tag{3.10}$$

$$+\frac{\langle\theta_o\rangle / L_y}{\left(1-\frac{\mu\delta_T}{2}\right)}\left(e^{-\mu x_e}-1\right)\sum_{n=1}\{e^{-2X/\delta_T}e^{-2nx_e} - e^{-t/\delta_T}e^{-\mu(X-t/2)}e^{-\mu nx_e}\}H(t-2X-2nx_e)$$

$$+\frac{\delta V_o}{L_y}\sum_{n=0}e^{-2X/\delta_T-2nx_e/\delta_T}\left[1-e^{-a(t-2X-2nx_e)}\right]H(t-2x-2nx_e)$$

The analogous result for the interior vertical velocity is given in Appendix A.

In (3.10) the notation *H(p)* stands for the Heavyside function which is zero for $p < 0$ and one for $p > 0$. I have also chosen a time dependence for the switch-on for the cross perimeter flow,

$$\delta V(t) = \delta V_o(1-e^{-at}) \tag{3.11}$$

to make the switch-on smooth and gradual. It is useful to examine (3.10) in detail.

The first square bracket on the right hand is the direct response to the buoyancy forcing under the assumption that the interface height on the eastern boundary is frozen at its zero initial position while the remaining terms are the consequence of the generation of Rossby wave activity excited by the interface motion on the eastern boundary as represented by (3.8). The first term is initially zero and reaches a steady state after a

single baroclinic Rossby wave crosses the basin in a time $T=2x_e$. That response is supplemented by the response of the interior to Rossby wave activity generated on the eastern boundary and is given by the remaining terms proportional to both the y integral of the buoyancy forcing as well as the net cross perimeter flow. These extra terms consist of three parts. The first is a term due to the buoyancy forcing which comes into steady equilibrium after the passage of a single baroclinic Rossby wave. However, if μ is not zero, that is if the forcing is non-uniform zonally, (and it does not matter whether μ is positive or negative) an infinite sequence of low frequency basin modes are excited. These are the modes discussed by LaCasce (2000), Cessi and Primeau (2001) and they are present in the wind -forced problem discussed by Cessi and Louazel (2001). It is important to note that the sums in (3.10) are finite since if $t - 2X < 2nx_e$ the Heavyside functions vanish. It is also possible to demonstrate that the appearance of each new Rossby wave at the eastern boundary at $t = 2nx_e$, occurs with a smaller amplitude as each signal decays at the rate δ_T^{-1}. Nevertheless, the time required for the basin to reach an equilibrium is not the crossing time a single Rossby wave but rather the damping time of the low frequency, baroclinic Rossby modes and as the previous studies already referenced have shown, these modes are very weakly damped. That being the case, the long time required to reach equilibrium implies that the basin will rarely exist in the equilibrium state unless the Rossby mode damping time is small. Each new disturbance will excite the weakly damped modal response.

For the simple quasi-geostrophic model here the unforced, normal mode solutions of (3.4) are:

$$\eta = N_e e^{i(kX-\omega t)} e^{-t/\delta_T},$$

$$k_j = 2j\pi / x_e, \quad j = 1,2,... \qquad \text{(3.12 a, b, c)}$$

$$\omega_j = k_j / 2$$

and satisfy the condition that the interface height be the same constant on the eastern and western boundaries. The poles of the factor in (3.9) will yield exactly the time behavior of the modes in (3.12) which is why the cancellation of this term when μ =0 expunges the Rossby wave behavior. Note that for all the non zero frequency modes a constant in x has no projection on those modes. Hence, a buoyancy forcing independent of x has no spatial projection on the Rossby low frequency basin modes, at least in the beta plane limit, and hence as we have noted from (3.10), those modes are not excited when μ =0. It is possible to show, considering the next term in an expansion in powers of *b*, that at next order in *b* the shift in the structure of the modes will produce a projection of zonally uniform forcing on the Rossby modes which will therefore be excited even by uniform forcing. It is also important to note that even in the quasi-geostrophic, beta-plane limit, the introduction of a time dependent cross perimeter flow will *always* excite the whole set of Rossby modes.

It is straightforward to show that the advancing fronts of the Rossby waves keeps the interface height continuous in x, although there are kinks across the front, while the interior vertical velocity w_i is *discontinuous* at the front of each Rossby wave. Figure 2 shows the response of the interior of the basin to a forcing of the form (3.4 b) with y_o =0, and with δ_T =2. For this value of δ_T the characteristic damping time for the Rossby wave due to vertical mixing is just equal to the transit time across the basin for x_e=1. In panel

2a the interface height at a position at the zonal mid-point of the basin is shown as a function of time. The heavy line is the full solution, the thin line shows that part of the solution corresponding to the solution with fixed, zero interface height at the eastern boundary. This latter, partial solution reaches a steady state after a single wave passage while the full solution requires the passage of several Rossby waves before it asymptotes to its final state. Note that the kinks in the curve correspond to the passage of a new wave front. In panel 2b the interface height is shown as a function of x for t =3. Since the time for the Rossby wave to traverse the basin is just 2 time units the kink in the curve at x=0.5 is the consequence of a second passage of a Rossby mode. Figure 3 shows the interior vertical velocity. Panel 3a shows w_i as a function of time at the same point as in Figure 2. Once again the full solution is shown by the heavy line and the solution that ignores the forcing by the eastern boundary is shown by the thin line. The full solution again takes much longer to equilibrate and shows a continuing arrival of jumps in the vertical velocity field as each Rossby wave front passes the observation point. The panel 3b shows the vertical velocity at t =3 as a function of longitude and the jump in vertical velocity of the full solution is very clear.

If the basin is not isolated but is subject to an inflow (or outflow) the basin modes will be excited even if the forcing is zonally uniform. Figure 4 shows the response of the interface in panel a) and the vertical velocity in panel b) at x=0.5 for δV= -0.5 (i.e. inflow). The dot-dashed curve in each figure shows the effect of the inflow on the solution and it is dominant. It is important to note that the inflow is the *net* inflow, integrated around the basin. Its effect is independent of the position of the inflow and the inflow is small, of *O(b)* the beta-plane parameter $\beta L / f_o$.

If δ_T is decreased the modes damp more rapidly and the discontinuities in the interior *w* field are much less evident. Indeed for very small values of δ_T only the first Rossby wave is can be clearly seen.

On the other hand, the *integral* of the interior vertical velocity across the zonal extent of the basin is, from (3.1. a) and (3.2)

$$\frac{1}{b}\int_0^{x_e} w_i dx = \frac{\left[\theta_o - \langle\theta_o\rangle / L_y\right]}{2\left(1-\mu\delta_T/2\right)}\left[\begin{array}{l} e^{-2x_e/\delta_T} - e^{-\mu x_e} \\ \\ +\left\{e^{-t/\delta_T} e^{\mu(t/2-x_e)} - e^{-2x_e/\delta_T}\right\}\left\{1-H(t-2x_e)\right\}\end{array}\right] \tag{3.13}$$

$$+\frac{\delta V_o}{L_y}(1-e^{-at})$$

and so the *net vertical velocity* on each latitude circle reaches a steady state after the first passage of a baroclinic Rossby wave across the basin. This follows from the form of the basin mode (3.12a). Since the average in x of the basin mode's vertical velocity is zero the series of modes required to place the interior in its final state adds nothing to the *net* upwelling on each latitude circle. This will somewhat alter in the planetary geostrophic approximation or in the presence of an irregular basin shape but that is beyond the scope of the present paper.

4) The boundary layer structure.

The boundary layers needed to complete the solution can be shown to be the same as those described in detail in PS so the discussion in this paper will be brief. In PS the boundary layers had a double structure. On the western boundary there is an outer layer whose width is δ_K (2.6) that closes the horizontal circulation and in which the flow continues to satisfy the Sverdrup balance, (3.2) . The neglect of the time derivatives in

(2.1 a, b) and (2.4) for that layer depends on the smallness of the parameter $b\varepsilon^2 / \delta_K$ which, in dimensional units is,

$$\frac{\beta L}{f_o}\frac{L_d^{\,2}}{L^2} = (\cot\theta)\frac{L_d^{\,2}}{\delta_{K*}R} \qquad (4.1)$$

where R is the earth's radius, δ_{K*} is the dimensional width of the boundary layer, and θ_O is the central latitude of the beta plane. As long as the western boundary layer is not much smaller than the deformation radius, the factor L_d / R guarantees that this term is negligible. Similarly, in (2.4) the smallness of δ_K / δ_T guarantees that the equation for the vertical velocity in the western boundary layer is simply,

$$w_i = -b\delta_K \eta_{xx} \qquad (4.2)$$

The neglect of those time derivatives renders the δ_K layer quasi- steady and its time dependence just responds parametrically to the time dependence imposed upon it by matching to the interior. As shown in PS the role of the δ_K layer is to satisfy the no-normal flow condition on x =0, or equivalently, to ensure that the interface height on the western boundary is the same as on the eastern boundary. If we write the total solution in the layer as the sum of the interior, here denoted with a subscript I, and a boundary layer correction denoted with a caret, the boundary condition is, for the correction function,

$$\eta_I(0,y,t) + \hat{\eta}(0,y,t) = N_e(t) \qquad (4.3)$$

or,

$$\hat{\eta}(0,y,t) = N_e - \eta_I(0,y,t) = \int_0^{x_e} \frac{\partial \eta_I}{\partial x} dx = \frac{2}{b} \int_0^{x_e} w_i dx \qquad (4.4)$$

and as we have seen in (3.13), this implies that the amplitude of the boundary layer interface height will come into a steady equilibrium after a single passage of a baroclinic Rossby wave since all variables in the boundary layer are proportional to $\hat{\eta}(0,y,t)$. This means in turn that the western boundary layer will come into equilibrium *before* the interior, a rather counterintuitive result. Since the Sverdrup balance (3.2) holds for the δ_K layer the net vertical transport in the layer at each latitude is equal and opposite to the integrated vertical velocity in the interior just as in PS even though the interior is time dependent. Its magnitude is given by (3.13) with opposite sign. Interior to the δ_K layer is the thinner hydrostatic layer described in PS. Its width is $\delta_h = \delta_K \left(\frac{\delta_m}{\delta_K} \right)^{3/2}$ and so is much thinner that the δ_K layer. In that layer the balances also do not involve the time derivatives in (2.1) and (2.4) and the vertical velocity is still given by (4.2) . Because of the insulating condition on the boundary the x-integral of the vertical velocity in this sub-layer must be equal and opposite to the vertical velocity in the δ_K layer and since the sub-layer is thinner the vertical velocity must be largest here. Again, in the sub-layer the motion will reach a steady state after as single passage of a baroclinic Rossby wave across the basin. Thus, as far as the vertical transports in the boundary layers are concerned, a single wave passage is all that is required for the results of PS to be valid even though the interior is till distant from equilibrium and this is due to the absence, in the quasi-geostrophic beta-plane model, of a net vertical motion along latitude circles in the Rossby basin modes. Indeed, *at each instant of time*, and at each latitude, the vertical

transport in the δ_K layer is equal and opposite to the interior's and in turn is balanced by the vertical transport in the δ_h layer.

5) Periodic solutions

Instead of examining the response of the basin to an abrupt switch-on of the buoyancy forcing this section describes the response to a sustained periodic forcing with the same spatial structure of the previous sections, i.e. we now take

$$\theta = \theta_o(y) e^{-\mu X} e^{-i\omega t} \qquad (5.1)$$

where ω is O(1) an order one frequency in units of time scaled with the Rossby basin mode period $T = L/\beta L_d^2$ and the real part of the above expression is intended. A solution valid in the interior and in the boundary layers in which the horizontal flow is closed is easily found using the method described in PS. In this solution (3.2) remains valid and the full representation (2.4) is used leading to the governing equation,

$$\nabla^2\eta + \frac{\eta_x}{2\delta_K} - \frac{\eta}{\delta_T\delta_K} - \frac{\eta_t}{\delta_K} = -\frac{\theta_o(y)}{\delta_T\delta_K} e^{-\mu X - i\omega t},$$

$$\theta_o = \theta_{oo}\left(\frac{y - y_o}{L_y}\right) \qquad (5.2, \text{a. b})$$

The solution that satisfies $\eta = N_e e^{-i\omega t}$ on all the lateral boundaries and determines N_e is given in Appendix B.

Figure 6 shows the real and imaginary parts of the interface height at t=0, and all subsequent times are, of course, a periodic evolution between these forms. In this calculation the frequency is chosen as the first normal mode frequency, i.e. $\omega = \pi$, and

otherwise the parameters are as in Figure 2. The shapes reflect the increased forcing in the northern part of the basin and the stronger, but narrow boundary layer required to satisfy the no-normal flow condition on the boundary. Qualitatively, however, the form of the response is that of the low frequency basin modes found by LaCasce (2000) and Cessi and Primeau (2001). The response remains sensitive to the cross perimeter flow into the basin and Figure 7 shows the response for the same parameter settings as in Figure 6 but now δV_o= -0.5.

Figure 8 shows the real and imaginary parts of the vertical velocity on the line y = 2(the mid-line of the basin) in the combined region of the interior plus the δ_K layer on the western boundary. The enhanced vertical velocity on the western boundary is evident. Its integral in x, i.e. the vertical transport in the δ_K layer balances the total vertical transport in the interior at all t as shown by (4.4). Not shown is the even larger vertical velocity in the very narrow δ_h layer whose transport is equal and opposite to the transport of the δ_K layer as in PS.

Figure 9 shows the amplitude of the interface deviation at the eastern boundary of the basin for the parameters of Figure 2 as a function of forcing frequency showing resonant peaks at the frequencies of the Rossby basin modes.

6. Discussion and conclusions.

A linear, quasi-geostrophic two-layer model is used to describe the time dependent response of a beta-plane basin to time dependent buoyancy forcing. In the model the vertical velocity at the interface is parameterized in terms of the departure of the interface from a prescribed spatial distribution. This represents the effect of vertical mixing and the

relaxation to the prescribed distribution acts as the buoyancy forcing. Lateral diffusion of layer thickness represents the effects of unresolved eddy fluxes of thickness.

When a steady forcing is switched on and when, and only when, the forcing has a non trivial dependence on longitude a spectrum of low frequency, weakly damped Rossby basin modes is excited and the interior of the basin does not come into steady state until the Rossby modes damp by vertical mixing. During the adjustment process Rossby wave fronts sweep across the basin and the interior vertical velocity is discontinuous across the fronts. The longitudinally averaged vertical velocity reaches a steady state after the passage of a single Rossby mode while the departure from the average requires a much longer time to reach steady state.

The net sinking is strongest in the western boundary layers and these layers come into equilibrium after the passage of the first Rossby wave mode. Thus, the sinking motion in the boundary layers comes into equilibrium before the local vertical velocity in the interior. This implies a non-local relation between the sinking, strongest in the western boundary layer and the buoyancy forcing. The response is particularly sensitive to the presence of a weak cross-perimeter baroclinic mass flux.

When the forcing is periodic the basin can resonate with the Rossby basin modes when the frequency of the forcing matches one of the Rossby modes. However, if there is no cross-perimeter flux and if the forcing is independent of longitude the resonance disappears.

The sensitivity of the response, in particular the time required to come to a steady state, to the spatial structure of the forcing and its relation to the Rossby basin modes emphasizes the important role these modes play in the buoyancy driven circulation. In all

cases the strongest sinking velocities occur in the western boundary layer, in particular in the narrow hydrostatic layer discussed in detail in PS. This sinking more rapidly comes into equilibrium with the forcing than the interior vertical velocity.

It will be of interest to extend these results to more realistic parameter settings in which nonlinearity, especially due to the action of meso-scale eddies, are important.

Acknowledgement. This research was supported in part by NSF grant OCE-9901654,

APPENDIX A

THE SOLUTION FOR THE INTERIOR VERTICAL VELOCITY.

From (3.2), (3.7) and (3.8) we obtain for the Laplace transform of the interior vertical velocity $\tilde{w}_i$,

$$\begin{aligned}\frac{\tilde{w}_i}{b} &= \frac{1}{2}\tilde{\eta}_x \\ &= \frac{1}{2}\frac{\theta_o(y)}{\delta_T s\left(s-\mu/2\right)+1/\delta_T)}\left[\mu e^{-\mu X} - 2(s+1/\delta_T)e^{-2(s+1/\delta_T)X}\right] \\ &+ \frac{\langle\theta_o\rangle / L_y}{\delta_T s\left(s-\mu/2\right)+1/\delta_T)}\left[e^{-\mu x_e} - e^{-2(s+1/\delta_T)x_e}\right]\frac{(s+1/\delta_T)e^{-2(s+1/\delta_T)X}}{1-e^{-2(s+1/\delta_T)x_e}} \\ &+ \frac{\delta\tilde{V}}{1-e^{-2(s+1/\delta_T)x_e}}(s+1/\delta_T)e^{-2(s+1/\delta_T)X}\end{aligned} \tag{A.1}$$

The representation in the time domain can be obtained by the same inversion method used for η or directly from (3.2) and (3.10) and is, the quasi-geostrophic beta-plane model for the Rossby basin modes to contain a net vertical velocity along a latitude circle.

(A.2)

$$\frac{2w_i}{b}=\frac{\theta_o}{(1-\mu\delta_T/2)}\left[\mu e^{-\mu X}\left\{1-e^{-t/\delta_T(1-\mu\delta_T/2)}\right\}-\left\{\frac{2}{\delta_T}e^{-2X/\delta_T}-\mu e^{-t/\delta_T}e^{-\mu(X-t/2)}\right\}\right]H(t-2X)$$

$$+\frac{\langle\theta_o\rangle/L_y}{(1-\mu\delta_T/2)}\sum_{n=0}\left[\begin{array}{l}e^{-\mu x_e}\left\{\frac{2}{\delta_T}e^{-2X/\delta_T-2nx_e/\delta_T}-\mu e^{-t/\delta_T}e^{-\mu(X-t/2)}e^{-n\mu x_e}\right\}H(t-2X-2nx_e)\\ -\left\{\frac{2}{\delta_T}e^{-2X/\delta_T}e^{-\mu(X-t/2)-2(n+1)x_e}-\mu e^{-t/\delta_T}e^{-\mu(X-t/2)-(n+1)\mu x_e}\right\}H(t-2X-2(n+1)x_e)\end{array}\right]$$

$$+\frac{\delta V_o}{L_y}\sum_{n=0}\left[\frac{2}{\delta_T}e^{-2X/\delta_T-2nx_e/\delta_T}\left(\left\{1-e^{-a(t-2X-2nx_e}\right\}+2ae^{-a(t-2X-2nx_e}\right)\right]H(t-2X-2nx_e)$$

APPENDIX B

THE SOLUTION OF (5.2) FOR PERIODIC FORCING

The solution of (5.2 a) for periodic, harmonic forcing when the buoyancy forcing is given by (5.1) and (5.2b) can be written,

$$\eta=\frac{\theta_o(y)}{D}\left[e^{-\mu X}-e^{X/4\delta_K}\frac{\sinh\alpha x}{\sinh\alpha x_e}-e^{-x/4\delta_K}e^{-\mu x_e}\frac{\sinh\alpha X}{\sinh\alpha x_e}\right]e^{-i\omega t}$$

$$+N_e\left[e^{X/4\delta_K}\frac{\sinh\alpha x}{\sinh\alpha x_e}+e^{-x/4\delta_K}\frac{\sinh\alpha X}{\sinh\alpha x_e}\right]e^{-i\omega t}+\Phi e^{-x/4\delta_K} \qquad \text{(B.1)}$$

where,

$$D = (1 - \mu\delta_T / 2 - \mu^2\delta_T\delta_K - i\omega\delta_T),$$

$$X = x_e - x, \qquad \text{(B. 2, a.b.c)}$$

$$\alpha = \frac{1}{4\delta_K}\left(1 + 16\frac{\delta_K}{\delta_T} - 16i\omega\delta_T\right)^{1/2}$$

while the function Φ is used to satisfy the boundary condition $\eta = N_e^{-i\omega t}$ on y = 0 and L_y, and is given by,

$$\Phi = \sum_{n=1}^{\infty}\left\{A_n\frac{\sinh\gamma_n y}{\sinh\gamma_n L_y} + B_n\frac{\sinh\gamma_n(L_y - y)}{\sinh\gamma_n L_y}\right\}\sin k_n x,$$

$$k_n = n\pi / x_e, \qquad \text{(B. 3 a, b, c)}$$

$$\gamma_n = \left\{k_n^{\,2} + (4\delta_K)^{-2} + (\delta_T\delta_K)^{-1} - i\omega / \delta_K\right\}^{1/2}$$

where

$$A_n = \frac{2}{x_e}N_e k_n\left(1 - (-1)^n e^{x_e/4\delta_K}\right)\left[\frac{1}{k_n^{\,2} + (4\delta_K)^{-2}} - \frac{1}{k_n^{\,2} + \alpha^2}\right]$$

$$-\frac{2}{x_e}\frac{\theta_o(L_y)}{D}k_n\left[e^{-\mu x_e} - (-1)^n e^{x_e/4\delta_K}\right]\left[\frac{1}{k_n^{\,2} + (\mu + 1/4\delta_K)^2} - \frac{1}{k_n^{\,2} + \alpha^2}\right] \qquad \text{(B.4)}$$

and $B_n = A_n$ with $\theta_o(L_y) \to \theta_o(0)$. To determine the interface height on the boundary it is only necessary to use the form of the above solution valid in the interior since the

boundary layers contribute negligibly to the satisfaction of (2.8). The solution in the interior is, asymptotically,

$$\eta = \frac{\theta_o(y)e^{-i\omega t}}{(1-\mu\delta_T/2-i\omega\delta_T)}\left[e^{-\mu X} - e^{-2(1-i\omega\delta_T)X/\delta_T}\right] + N_e e^{-2(1-i\omega\delta_T)X/\delta_T} e^{-i\omega t}, \qquad \text{(B.5)}$$

and the application of (2.8) yields,

$$N_e = \frac{\langle\theta_o\rangle / L_y}{\left(1-\mu\delta_T/2-i\omega\delta_T\right)} \frac{\left[e^{-\mu x_e} - e^{-2(1-i\omega\delta_T)x_e/\delta_T}\right]}{\left[1-e^{-2(1-i\omega\delta_T)x_e/\delta_T}\right]} \qquad \text{(B.6)}$$

which completes the solution.

References

Cessi, P. and F. Primeau, 2001. Dissipative selection of low-frequency modes in a reduced-gravity basin. *J. Phys. Ocean.*, **31**, 127-137.

_____ and S. Louazel, 2001. Decadal ocean response to stochastic wind forcing. *J. Phys. Ocean.*, **31**, 3020-3029.

Gent. P.R. and J.C. McWilliams, 1990. Isopycnal mixing in ocean circulation models. *J. Phys. Ocean.* **20**, 150-155.

LaCasce, J. H., 2000. Baroclinic Rossby waves in a square basin. *J. Phys. Ocean.,* **30**, 3161-3178.

_____ and J. Pedlosky. 2002. Baroclinic Rossby waves in irregular basins. *J. Phys. Ocean.,* **32**, 2828-2847.

Lucas, M.A. , J.J. Hirsch, J.D. Stark and J. Marotzke, 2005. The response of an idealized ocean basin to variable buoyancy forcing. *J. Phys. Ocean.*, **35**, 601-615.

Pedlosky, J. and M. A. Spall, 2005. Boundary intensification of vertical velocity in a beta-plane basin. *J. Phys. Ocean.* (accepted for publication).

Figure Captions

Figure 1. The two-layer model. a) A view of the layers in elevation. The vertical velocity at the interface, w_i is composed of a cross-isopycnal velocity and the motion of the interface. The cross isopycnal velocity is positive when heavy water is transformed to lighter water. b) The basin in plan view. A small non quasi-geostrophic velocity is allowed to leave (or enter) the basin.

Figure 2. The response of the interface for δ_T =2, μ=2, δV=0, a=4, L_y=4, x_e=1,y_0 =0. a) η as a function of time for x=0.5. b) The interface height at t=3 as a function of x. See text for discussion.

Figure 3. The interior vertical velocity for the same parameter settings as Figure 2. a) w_i as a function of t at the same position as in Figure 2. b) As a function of x at t =3.

Figure 4. a) $\eta(t)$ mid-way across the basin for the parameters of Figure 2 but for δV=-0.5. b) The same settings showing the vertical velocity as a function of time. In each panel the dot-dash line shows the contribution from the cross perimeter flux.

Figure 5. As in Figure 4 except that δ_T is now 0.25. The interior equilibrates after the passage of a single Rossby wave.

Figure 6. The real and imaginary parts of the solution for periodic forcing at frequency $\omega = \pi$. The parameter settings are otherwise as in Figure 2. The heavy lines are the zero contours of real and imaginary η.

Figure 7. The response of the basin to periodic buoyancy forcing as in Figure 6 but with δV_o=-0.5.

Figure 8. The profiles on y=2 of the real and imaginary parts of $2w_i/b$ for the parameters of Figure 6. Note the enhanced vertical velocity in the western boundary layer.

Figure 9. The magnitude of η on the eastern boundary as a function of frequency for the parameters of Figure 4.

a)

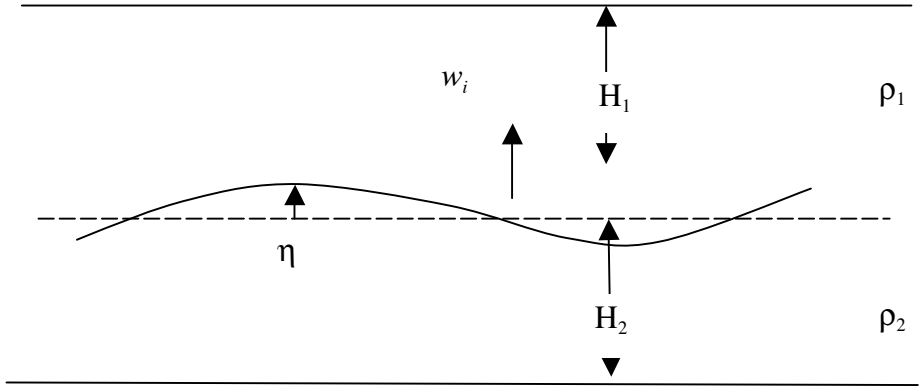

b)

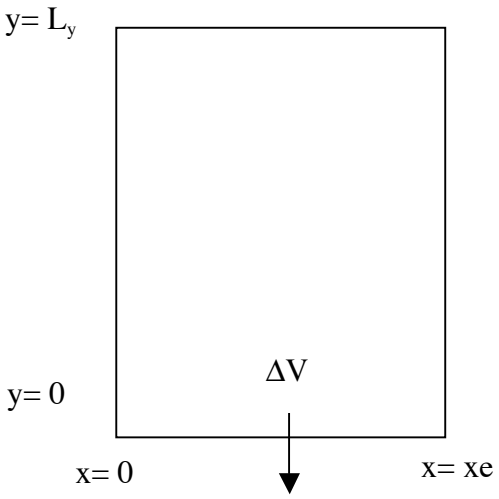

Figure 1. The two-layer model. a) A view of the layers in elevation. The vertical velocity at the interface, w_i is composed of a cross-isopycnal velocity and the motion of the interface. The cross isopycnal velocity is positive when heavy water is transformed to lighter water. b) The basin in plan view. A small non quasi-geostrophic velocity is allowed to leave (or enter) the basin.

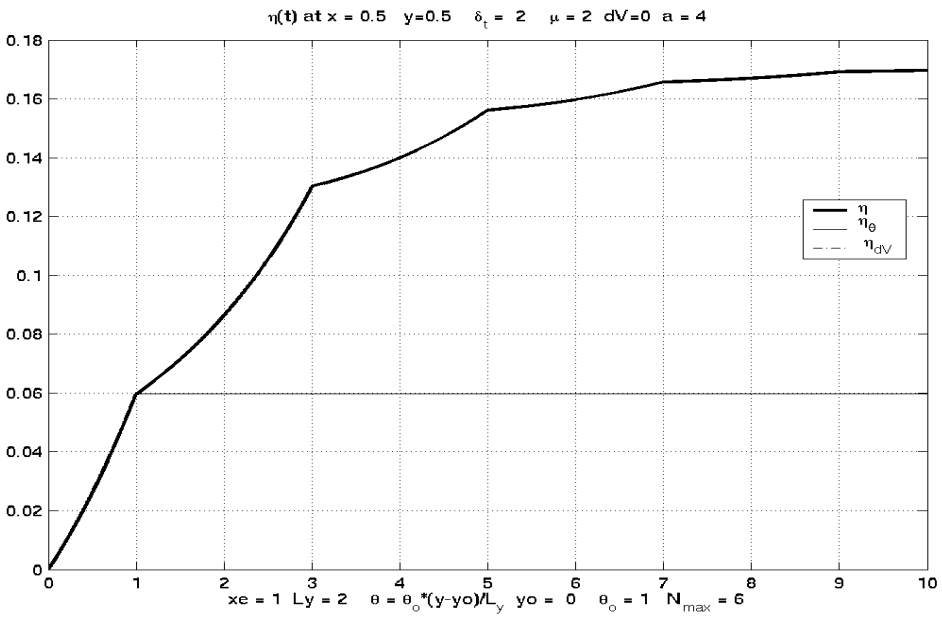

a)

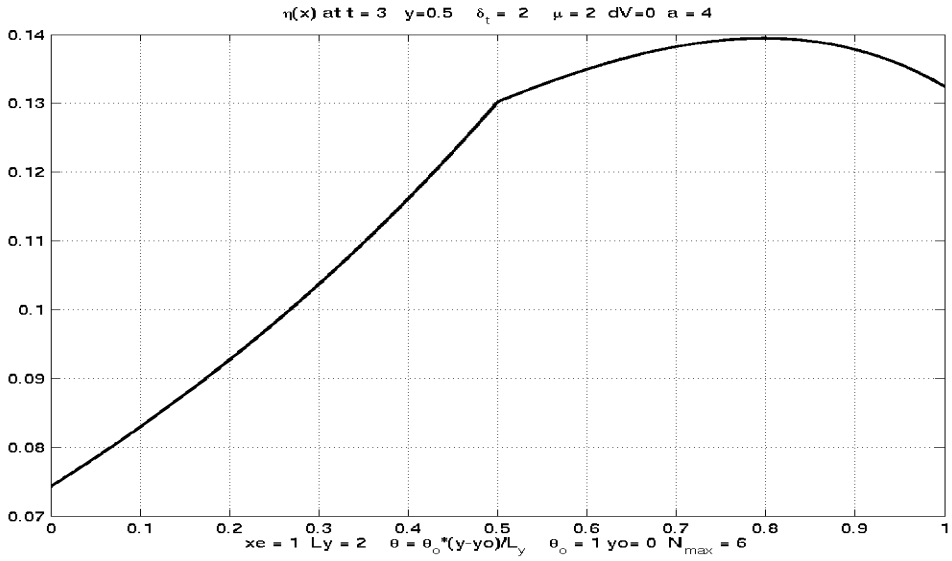

b)

Figure 2. The response of the interface for δ_T =2, μ=2, dV=0, a=4, L_y=4, x_e=1, y_o=0. a) η as a function of time for x=0.5. b) The interface height at t=3 as a function of x.

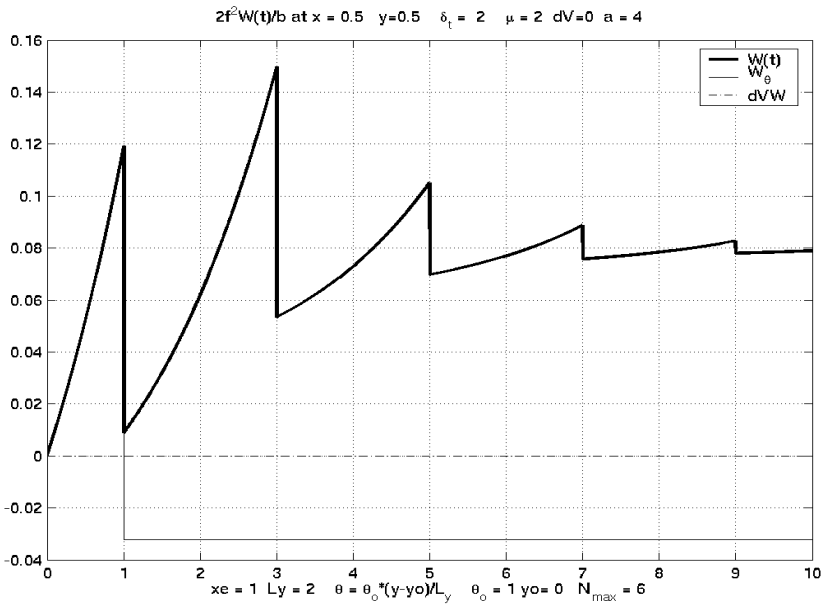

a)

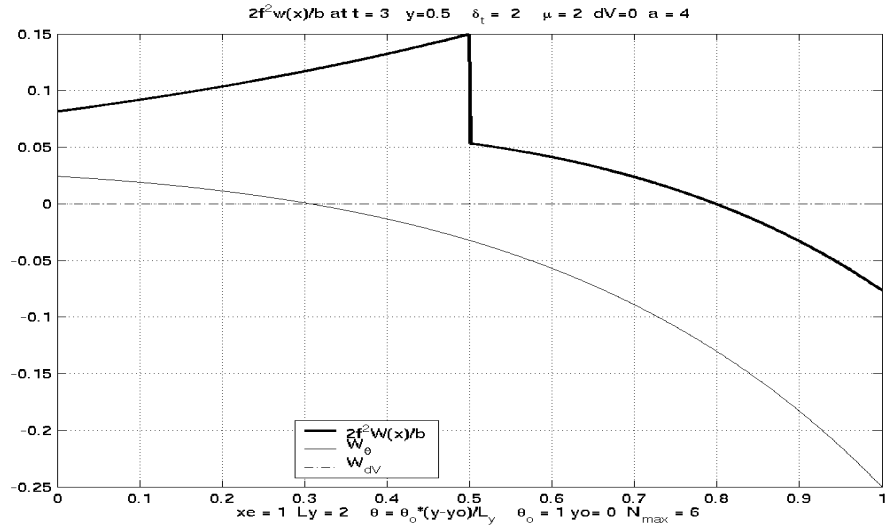

b)

Figure 3. The interior vertical velocity for the same parameter settings as Figure 2. a) w_i as a function of t at the same position as in Figure 2. b) As a function of x at t =3.

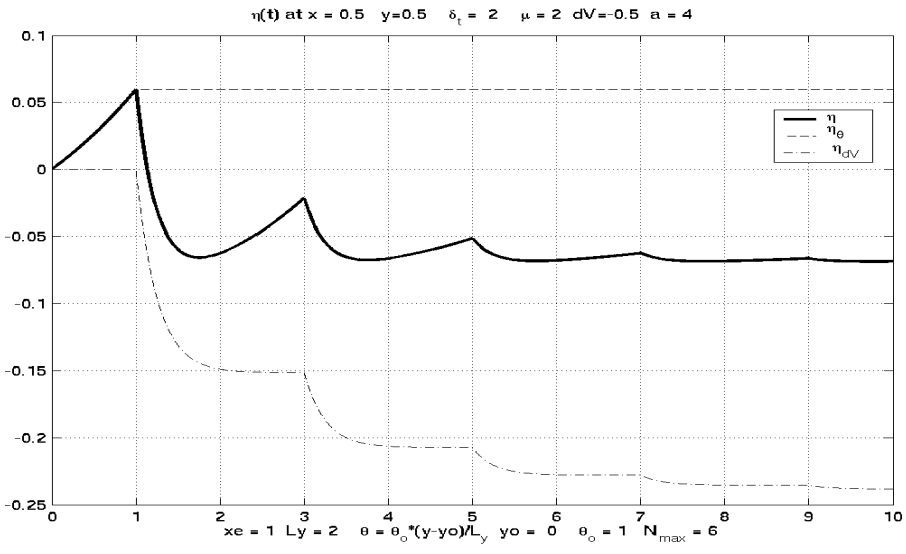

a)

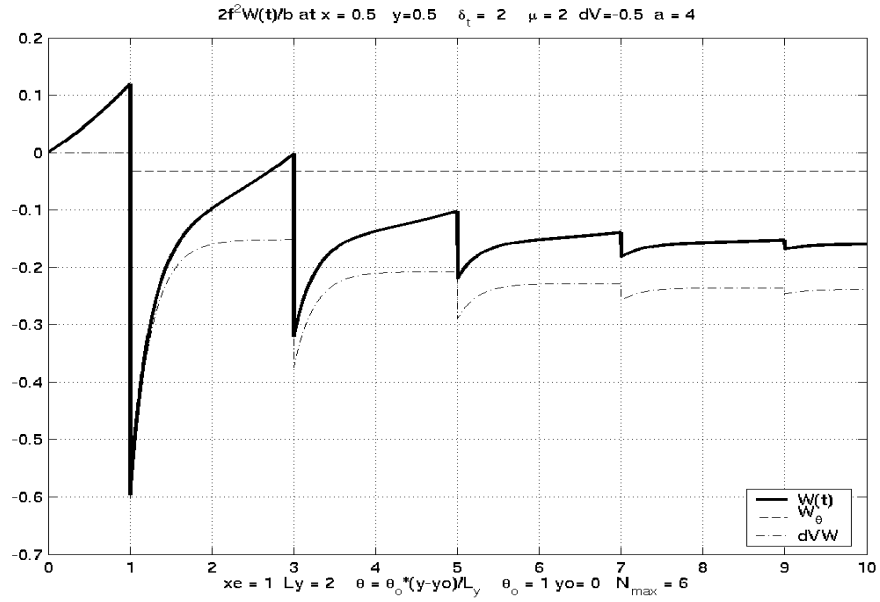

b)

Figure 4. a) $\eta(t)$ mid-way across the basin for the parameters of Figure 2 but for δV=-0.5. b) The same settings showing the vertical velocity as a function of time. In each panel the dot-dash line shows the contribution from the cross perimeter flux.

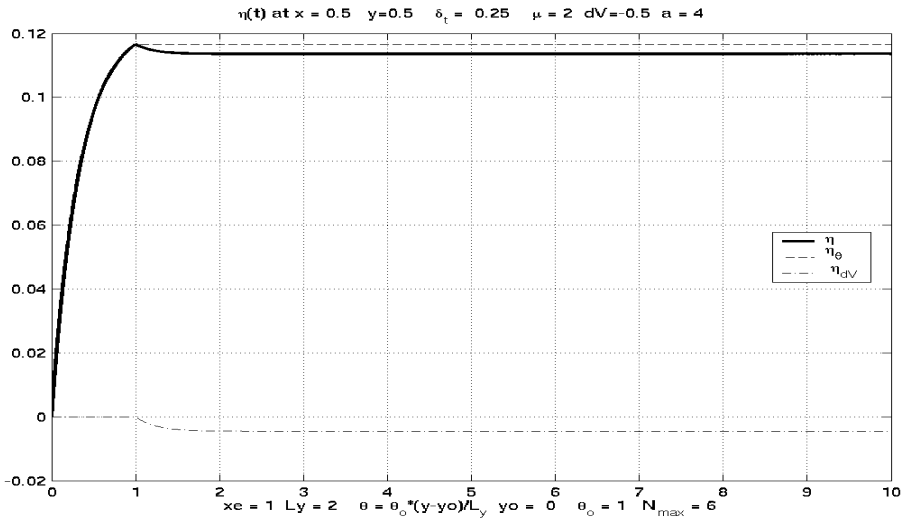

a)

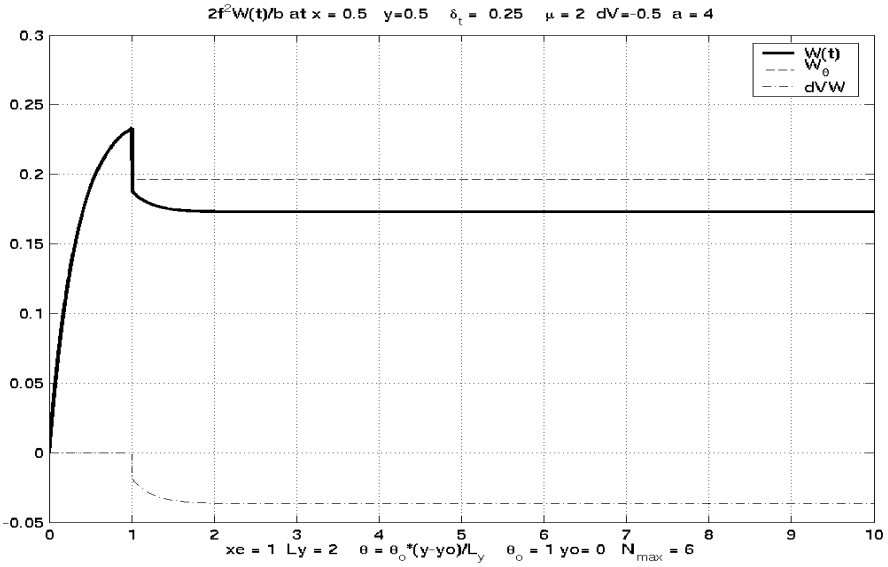

b)

Figure 5. As in Figure 4 except that δ_T is now 0.25. The interior equilibrates after the passage of a single Rossby wave.

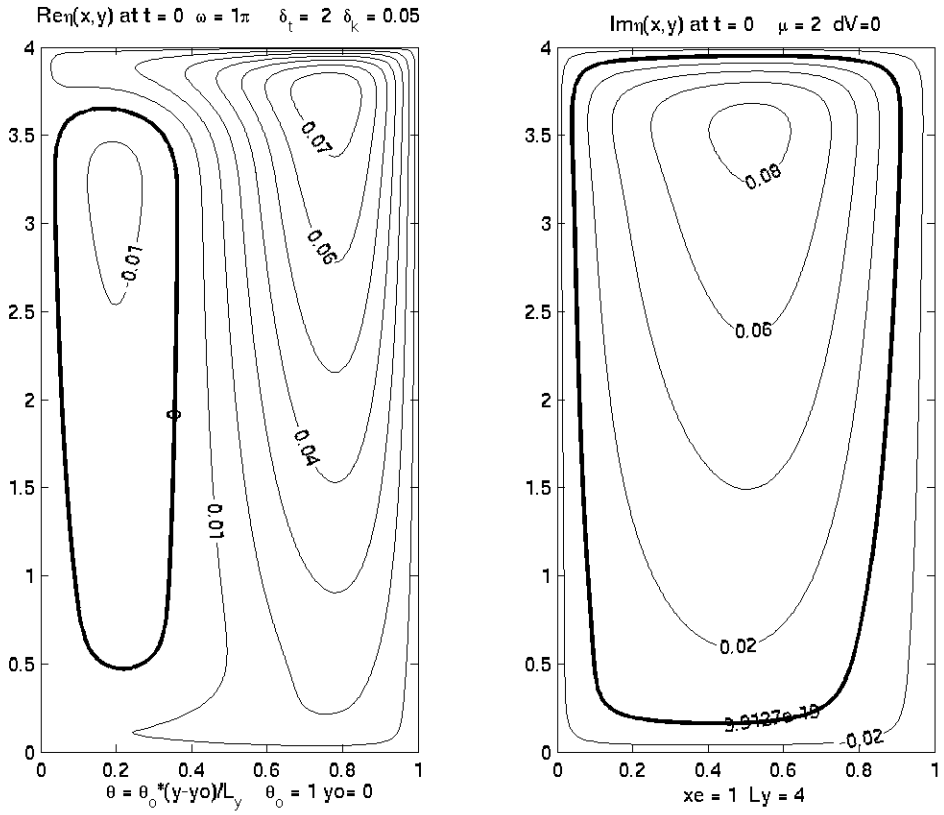

Figure 6. The real and imaginary parts of the solution for periodic forcing at frequency $\omega = \pi$. The parameter settings are otherwise as in Figure 2. The heavy lines are the zero contours of real and imaginary η.

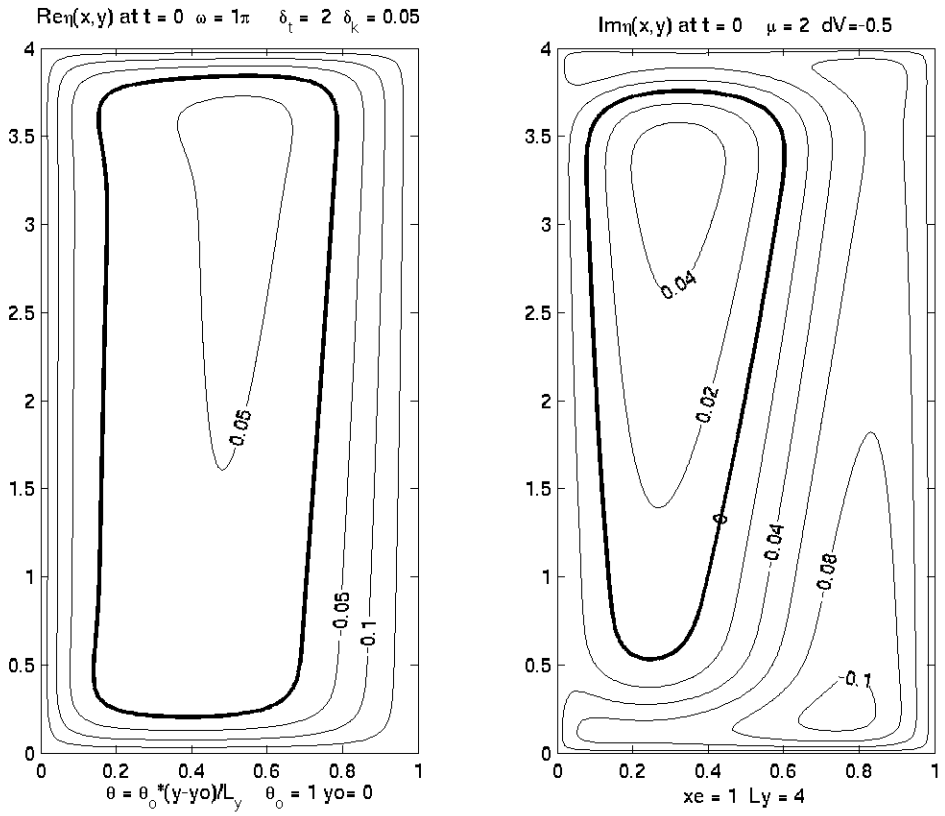

Figure 7. The response of the basin to periodic buoyancy forcing as in Figure 6 but with δV_o=-0.5

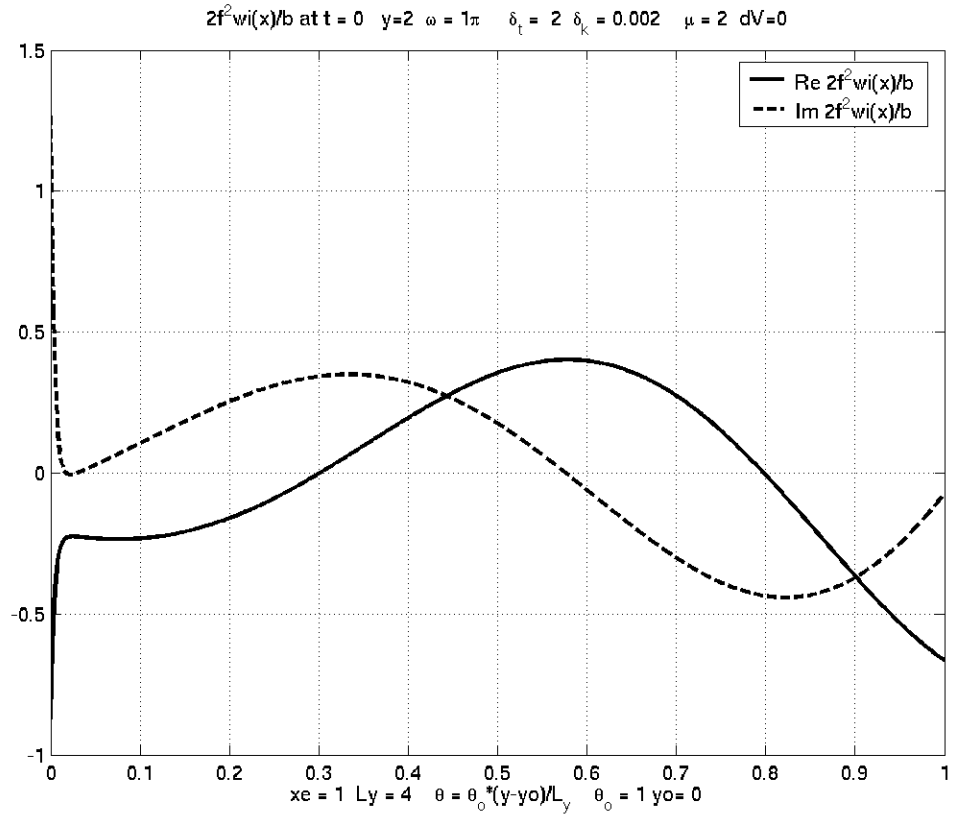

Figure 8. The profiles on y=2 of the real and imaginary parts of $2w_i/b$ for the parameters of Figure 6. Note the enhanced vertical velocity in the western boundary layer.

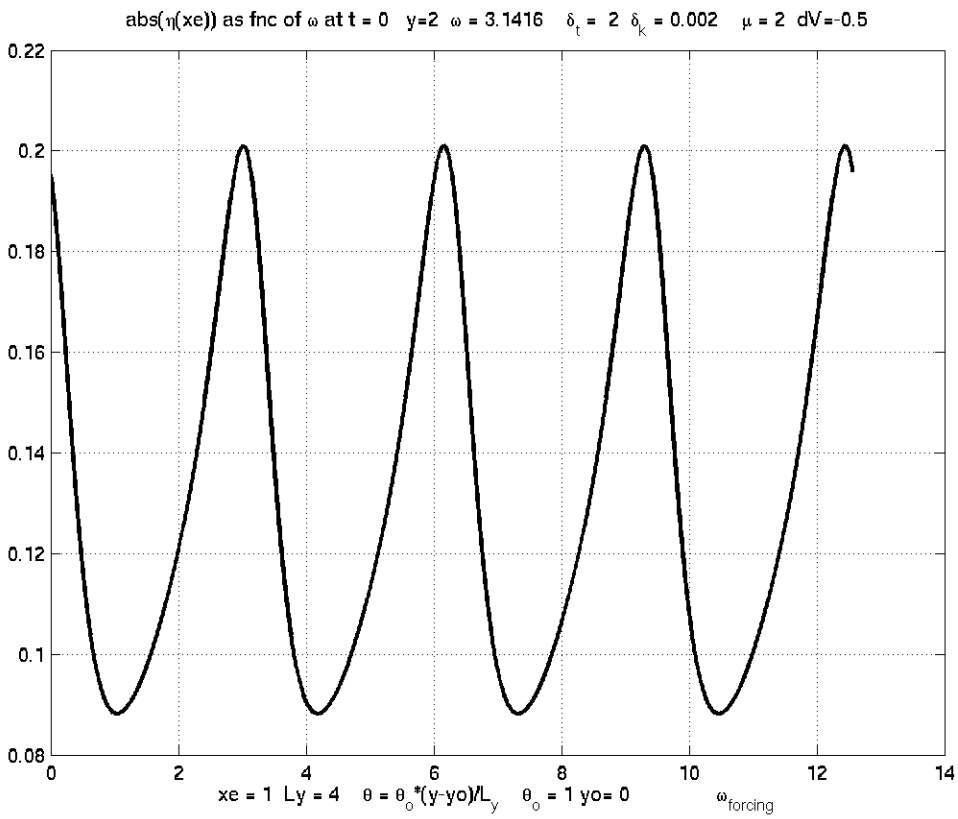

Figure 9. The magnitude of η on the eastern boundary as a function of frequency for the parameters of Figure 4.